ELSEVIER

Cancer Genetics and Cytogenetics 196 (2010) 45–55

Cancer Genetics and Cytogenetics

UOK 262 cell line, fumarate hydratase deficient (FH^{-}/FH^{-}) hereditary leiomyomatosis renal cell carcinoma: in vitro and in vivo model of an aberrant energy metabolic pathway in human cancer

Youfeng Yang[a], Vladimir A. Valera[a], Hesed M. Padilla-Nash[b], Carole Sourbier[a], Cathy D. Vocke[a], Manish A. Vira[a], Mones S. Abu-Asab[c], Gennady Bratslavsky[a], Maria Tsokos[c], Maria J. Merino[c], Peter A. Pinto[a], Ramaprasad Srinivasan[a], Thomas Ried[b], Len Neckers[a], W. Marston Linehan[a,*]

[a]*Urologic Oncology Branch, Center for Cancer Research, National Cancer Institute, National Institutes of Health, 10 Center Dr., MSC 1107, Bldg 10 CRC, Room 1-5942, Bethesda, MD 20892-1107*

[b]*Genetics Branch, Center for Cancer Research, National Cancer Institute, National Institutes of Health, Bethesda, MD 20892*

[c]*Laboratory of Pathology, Center for Cancer Research, National Cancer Institute, National Institutes of Health, Bethesda, MD 20892*

Received 29 July 2009; accepted 27 August 2009

Abstract Energy deregulation and abnormalities of tumor cell metabolism are critical issues in understanding cancer. Hereditary leiomyomatosis renal cell carcinoma (HLRCC) is an aggressive form of RCC characterized by germline mutation of the Krebs cycle enzyme fumarate hydratase (FH), and one known to be highly metastatic and unusually lethal. There is considerable utility in establishing preclinical cell and xenograft models for study of disorders of energy metabolism, as well as in development of new therapeutic approaches targeting of tricarboxylic acid (TCA) cycle enzyme–deficient human cancers. Here we describe a new immortalized cell line, UOK 262, derived from a patient having aggressive HLRCC-associated recurring kidney cancer. We investigated gene expression, chromosome profiles, efflux bioenergetic analysis, mitochondrial ultrastructure, FH catabolic activity, invasiveness, and optimal glucose requirements for in vitro growth. UOK 262 cells have an isochromosome 1q recurring chromosome abnormality, i(1)(q10), and exhibit compromised oxidative phosphorylation and in vitro dependence on anaerobic glycolysis consistent with the clinical manifestation of HLRCC. The cells also display glucose-dependent growth, an elevated rate of lactate efflux, and overexpression of the glucose transporter GLUT1 and of lactate dehydrogenase A (LDHA). Mutant FH protein was present primarily in edematous mitochondria, but with catalytic activity nearly undetectable. UOK 262 xenografts retain the characteristics of HLRCC histopathology. Our findings indicate that the severe compromise of oxidative phosphorylation and rapid glycolytic flux in UOK 262 are an essential feature of this TCA cycle enzyme-deficient form of kidney cancer. This tumor model is the embodiment of the Warburg effect. UOK 262 provides a unique in vitro and in vivo preclinical model for studying the bioenergetics of the Warburg effect in human cancer.

1. Introduction

Hereditary leiomyomatosis and renal cell carcinoma (HLRCC) is an inherited cancer syndrome in which affected individuals are at risk for development of cutaneous and uterine leiomyomas and of renal cell carcinoma (RCC). The cutaneous and uterine manifestations [1] and the renal manifestations [2] were described as autosomal dominant conditions in 1995. In 2001 the cutaneous, uterine, and renal manifestations were described as a single entity by Launonen et al. [3], and the condition was renamed hereditary leiomyomatosis and renal cell carcinoma (HLRCC). Typically, HLRCC- associated renal lesions present as unilateral, solitary, high-grade tumors that have a predisposition to metastasize early [2,4–6].

The *FH* gene, which causes HLRCC, encodes fumarate hydratase (FH), one of the essential metabolic enzymes of the tricarboxylic acid (TCA) cycle (also termed the Krebs cycle), and has been mapped using linkage analysis to the

* Corresponding author. Tel.: (301) 496-6353; fax: (301) 402-0922.
E-mail address: wml@nih.gov (W.M. Linehan).

0165-4608/10/$ – see front matter
doi:10.1016/j.cancergencyto.2009.08.018

long arm of chromosome 1 at 1q42.3~q43 [4,7]. Previous reports have indicated that these tumors display papillary type 2 histology [7]. Merino et al. [8] described the unique features of HLRCC tumor cell morphology: not only a high Fuhrman grade (3 or 4) suggestive of papillary type 2 histological type, but also the presence of large eosinophilic nucleoli with a clear perinucleolar halo. Use of these unique morphologic features has greatly improved diagnostic accuracy for HLRCC kidney cancer.

Investigators have noted that a common feature of a number of types of cancer is preferential utilization and catabolism of glucose [9−15], particularly in tumors with high malignant potential, tumors that are poorly differentiated, and tumors that proliferate rapidly. Despite considerable progress in identification of the genetic and molecular factors contributing to the malignant phenotype of HLRCC, studies of gene and protein expression and of the cytogenetics of HLRCCs are limited, and there has been no well-characterized tumor cell line model available. We have previously established and characterized renal tumor cell lines for studies of the *VHL* gene in clear cell kidney cancer [16], the *FLCN* (alias *BHD*) gene in the Birt−Hogg−Dubé syndrome [17], and the *TFE3* gene [18,19].

This report describes the properties of the UOK 262 cell line, which was established from a metastatic HLRCC kidney tumor surgically removed from a patient with recurrent kidney cancer. Unlike other available renal carcinoma cell lines, UOK 262 cells provide both an in vitro and an in vivo model for studying the metabolic impact of fumarate hydratase deficiency in kidney cancer. This cell line provides a unique model with which to study the Warburg phenomenon in human cancer.

2. Materials and methods

2.1. Patient characteristics

The patient, who was evaluated at the U.S. National Cancer Institute (NCI) on a Urologic Oncology Branch protocol approved by the NCI institutional review board, gave written informed consent for participation in this study. The presentation and clinical course of this patient were described previously [6].

In brief, the patient was an asymptomatic 48-year-old white female who was initially found to have a large renal mass during an evaluation initiated because of a strong family history of renal cell carcinoma and because of cutaneous findings characteristic of HLRCC. The patient's past medical history was notable for presence of multiple cutaneous leiomyomas on arms and trunk, as well as uterine fibroids requiring myomectomy and partial hysterectomy at an early age. She underwent an open right radical nephrectomy of a 10-cm renal tumor at an outside institution. The renal pathology revealed a renal cell carcinoma with tubulopapillary and clear cell histology. The surgical margins were free of tumor.

Approximately 14 months after the initial surgery, the patient was found to have a tumor recurrence in the retroperitoneum and retroperitoneal lymphadenopathy, which suggested metastatic disease. Metastatic work-up revealed disease localized to the retroperitoneum. The patient underwent exploratory laparotomy and retroperitoneal lymph node dissection. Pathologic evaluation revealed the presence of the tumor in the right adrenal gland, as well as in four retrocaval nodes. Given the identification of cutaneous leiomyomata, the early onset of uterine fibroids, prior renal carcinoma, and a strong family history of kidney cancer, the patient underwent germline genetic testing to confirm the diagnosis of HLRCC. She was found to have a germline mutation in *FH*, the fumarate hydratase gene [6]. The patient was subsequently found to have disease progression in the mediastinum, as well as new lesions on the calvarium. Despite an initial response to systemic chemotherapy, the disease progressed further and the patient died ~21 months after her original renal surgery.

2.2. Establishment of the UOK 262 immortalized cell line

The UOK 262 cell line was established from tumor tissue following tissue and cell culture protocols and techniques of the Urologic Oncology Branch, as previously described, with modifications [17]. The first passage was carried out 2−3 days after plating by a light treatment with 0.05% trypsin−ethylene-diamine-tetraacetic acid, while monitoring the cells under an inverted tissue culture microscope. After passage 20, subsequent passages were carried out every 2−3 days by splitting 1 to 2 in the same manner.

2.3. Tumor xenografts in Nu/Nu nude mice

Animal usage was in accordance with the guidelines of the National Cancer Institute. Female athymic nude mice (Taconic, Germantown, NY) were received at 4−5 weeks of age and kept in our animal facility for 2 weeks prior to injection with tumor cells. Approximately 5×10^6 UOK 262 cells in 0.2 mL (50:50 1 × Hanks buffered salt solution−Matrigel [BD Bioscience, San Jose, CA]) were injected subcutaneously into athymic nude mice, in the right flank, to determine the tumorigenic potential, as previously described [17]. Xenograft tumor specimens were re-implanted into additional mice, grown, harvested, and this process was repeated several times.

2.4. Glucose dependence of cell growth in vitro

Growth rates were compared under conditions of low (0.5 g/L and 2.5 g/L) and high (5 g/L and 10 g/L) glucose in Dulbecco's modified Eagle's medium (DMEM; Invitrogen, Carlsbad, CA). Equal numbers of cells were plated into six-well plates at ~30% initial confluence and were allowed to grow for 72 hours. Cells in particular wells were counted in triplicate at 24-hour intervals using a Cellometer

auto T4 image-based cell counter (Nexcelom Bioscience, Lawrence, MA).

2.5. Measurements of extracellular acidification and oxygen consumption rate

The XF24 extracellular flux analyzer (Seahorse Bioscience, North Billerica, MA) was used to detect rapid, real-time changes in cellular respiration and glycolysis rate. UOK 262 and control cells (786–O and HK-2; ATCC, Manassas, VA) were cultured in custom XF24 microplates. Analysis of the extracellular acidification rate (ECAR) reflects lactate excretion and serves as an indirect measure of glycolysis rate; O_2 consumption (OCR) reflects cellular respiration and is directly determined [20]. All measurements were performed following manufacturer's instructions and protocols, and the observed rates are reported in pmol/min for OCR and mpH/min for ECAR.

2.6. Cell invasion assay

In vitro invasiveness of UOK 262 cells was evaluated using a cell invasion and migration monitoring system (RT-CIM; ACEA Biosciences, San Diego, CA) and was compared with both VHL-deficient 786–O clear cell renal carcinoma cells and HRCE normal renal cortical epithelial cells (catalog no. CC-2654; Lonza, Basel, Switzerland). The upper and lower culture compartments of the device are separated by a polyester membrane of 8 μm pore size coated with fibronectin (10 μg/mL). The membrane itself contains microelectronic sensor arrays that register an impedance signal as cells pass through from upper to lower chamber, which serves as a reservoir for media. Prior to assay, cells were cultured overnight without serum. The wells were filled with serum-free DMEM in the top chamber and with DMEM containing 10% fetal bovine serum in the bottom chamber. Both chambers were incubated for 30 minutes at 37°C. Then 4×10^4 cells of each cell line were added per well to the top chamber (serum free medium). All wells were prepared in triplicate and invasion was monitored in real time for 5 days in a humidified incubator at 37°C and 5% CO_2. Using software supplied by the manufacturer, we derived a dimensionless parameter, the cell index, to quantify the invasiveness of each cell line, and this value was plotted against incubation time.

2.7. Spectral karyotyping, gene-specific fluorescence in situ hybridization analysis, and DNA sequencing

The metaphase chromosomes were prepared from passage 16 of UOK 262 cells. Three bacterial artificial chromosome-based human genomic DNAs were used as gene specific probes for fluorescence in situ hybridization (FISH) analysis: from 5′ end, RP11-409K12 (70 kb); RP11-509A24 (4 kb); RP11-527D7(157 kb). The detailed methods for spectral karyotyping (SKY) and FISH analyses were as previously described [21,22]. The karyotype for UOK 262 (see section 3.4 and the figure cited therein) has been entered into the NCBI SKY/CGH interactive online database (http://www.ncbi.nlm.nih.gov/sky/skyweb.cgi). Public access takes effect upon publication of the present article. DNA sequencing was performed as previously described [17].

2.8. Cellular and ultrastructural imaging of mitochondria

Both UOK 262 cells and control HRCE human renal cortical epithelial cells were harvested in triplicate at passage 34. Cell pellet fixation and thin sectioning for ultrastructural studies was carried out as described previously [17] with minor modifications. The cell pellet was fixed in 2.5% phosphate-buffered saline (PBS)–buffered glutaraldehyde, postfixed in 1.0% osmium tetroxide in 0.1 mol/L sodium cacodylate buffer, dehydrated in a series of ethanol, and infiltrated with Epon–Araldite epoxide resin (Ted Pella, Redding, CA) for 2 days. Samples were polymerized at 60°C for 2 days. Ultrathin sections (~100 nm) were cut using a Leica EM UC6 Microtome (Leica Microsystems, Wetzlar, Germany; Bannockburn, IL) and collected on film-supported slot grids. Sections were slightly counter-stained with uranyl acetate and lead citrate, and examined with a Philips CM120 transmission electron microscope (equipped with a model GIF100 camera; Gatan, Pleasanton, CA) operating at a beam energy of 80 kV. Images were acquired by using a Gatan high-resolution charge-coupled device camera.

2.9. Antibodies, immunohistochemistry, and immunoblotting

UOK 262 cells (passage 16) were seeded in Lab-TEK II chamber slides (Nalge Nunc International, Naperville, IL), fixed in 3.7% formaldehyde in PBS, and permeabilized in 0.2% Triton-X100. Cells were then washed three times in PBS and incubated for 1 hour at room temperature with either rabbit anti-human GLUT1 (1:500 dilution; Dako, Glostrup, Denmark) or mouse anti-human FH (1:200 dilution; catalog no. ab58232, Abcam, Cambridge, UK). Antibodies used for mitochondria analysis include rabbit anti-human SOD2 (catalog no. ab13533; Abcam). After three washes in PBS, cells were incubated with either goat anti-rabbit or goat anti-mouse IgG-Alexa fluor 488/Alexa fluor 594 (1:500 dilution; Invitrogen) for 30 minutes at room temperature, washed in PBS, and briefly counterstained with 4′,6-diamidino-2-phenylindole.

After mounting, cells were observed under a Leica DMRxA fluorescent microscope and images were obtained with IPLab v.3.7 software (Scanalytics, Fairfax, VA). Antibodies used for Western blotting include β-actin (catalog no. A2522; Sigma–Aldrich, St. Louis, MO) and FH (catalog no. ab58232; Abcam).

2.10. Gene expression analysis by quantitative real-time polymerase chain reaction

Gene expression was analyzed by real-time polymerase chain reaction (PCR) for *FH* and four other genes: solute carrier family 2 (facilitated glucose transporter), member 1 (*SLC2A1*, 1p34.2; previously *GLUT1*); *LDHA*; succinate dehydrogenase complex, subunit C, integral membrane protein, 15 kDa (*SDHC*, 1q21); and peroxisome proliferator-activated receptor gamma, coactivator 1 alpha (*PPARGC1A*; alias *PGC1A*).

In brief, total RNA was extracted from 1.0×10^6 UOK 262 cells using TRIzol (Invitrogen). Total RNA (20 ng) was reverse-transcribed for cDNA synthesis using random hexamers in a final volume of 20 μL, and 1 μL of the resulting cDNA was used for PCR amplification in an ABI 7000 real-time PCR system (Applied Biosystems, Foster City, CA) as recommended by the manufacturer. Primers and fluorogenic probes were designed by Applied Biosystems in the form of TaqMan: assay no. Hs00197884_ml (for *SLC2A1*, alias *GLUT1*), Hs00855332_gl (*LDHA*), Hs00818427_ml (*SDHC*), and Hs00173304_m1 (*PPARGC1A*; alias *PGC1A*). mRNA expression for these genes in UOK 262 was normalized to the housekeeping gene peptidylprolyl isomerase A (cyclophilin A) (*PPIA*; alias *CYPA*) and CT values were further normalized to those obtained from a normal HRCE cell line. Samples were run in duplicate and CT values obtained were compared by the ΔCT method. Results are expressed as fold-change relative to HRCE values from two independent experiments.

2.11. Measurement of FH enzyme activity

Whole-cell protein quantification in the extract of UOK 262 and control cells was undertaken by the bicinchoninic acid colorimetric assay as previously described [23]. In vitro FH enzyme activity was measured by NADP−malic enzyme coupled assay as previously described [24]. In brief, the increase in absorbance at 340 nm from NADPH formation was measured after adding fumarate (Sigma−Aldrich) at final concentration of 10 mmol/L into a total volume of 1 mL reaction mixture of cell extract at 30 °C for 10 minutes. All spectrophotometric measurements were conducted using a Beckman DU-530 spectrophotometer (Beckman Coulter, Fullerton, CA).

3. Results

3.1. Glucose uptake by PET imaging in vivo and glucose dependence of cultured tumor cells in vitro

As we have described here, upon completion of the metastatic work-up the disease from the patient appeared to be localized to the retroperitoneum and was best viewed by abdominal and pelvic computed tomography (CT) as well as by positron emission tomography (PET). Anatomic imaging of the tumor mass was performed with CT (Fig. 1A). A regional lymph node metastasis was identified based on enhanced glucose uptake observed from PET imaging with fluorodeoxyglucose ([^{18}F]FDG) (Fig. 1B).

To determine if UOK 262 cells display increased glucose dependence in vitro, we monitored their growth in media containing concentrations of glucose varying from 0.5 to 10 g/L (Fig. 1C). In contrast to the clear cell RCC cell line 786−O, UOK 262 cells required a glucose concentration of at least 2.5 g/L for survival and at least 5 g/L for optimal growth.

3.2. Invasiveness of UOK 262 cells

UOK 262 cells in culture exhibited an atypical branching morphology, and histopathologic features notably similar to HLRCC, such as large nuclei with prominent nucleoli and atypical perinucleolar clearing (Fig. 1D). We next compared the in vitro invasive potential of UOK 262 with that of HRCE and 786−O cells. The real-time quantitative assessment of invasion for each cell line showed that UOK 262 was more invasive than 786−O, and untransformed HRCE cells were not invasive (Fig. 1E).

3.3. UOK 262 retains HLRCC histopathologic features

Histopathologic analysis of subcutaneous xenograft tumors (Fig. 2A) derived from UOK 262 revealed that UOK 262 retained the characteristic features of the retroperitoneal nodal HLRCC tumor (Fig. 2B) from which it was derived: both are characterized by large eosinophilic nuclei or nucleoli and atypical perinucleolar clearing [8]. These characteristics were noted in the patient's primary kidney tumor, as well as in a retroperitoneal lymph node metastasis (data not shown).

3.4. Cytogenetics and identification of isochromosome i(1)(q10) in UOK 262 cells

Three different DNA probes together encompassing the entire *FH* gene genomic region were used to determine gene copy number by FISH (Fig. 2C). Spectral karyotyping was also performed, to detect alterations at the chromosome level (Fig. 2D). FISH analysis showed that all three *FH* genomic DNA fragments from the bacterial artificial chromosome-based human genomic DNA (see section 2.7) are present in both the normal chromosome 1 and in an isochromosome 1, i(1)(q10), at band 1q42.3 (in UOK 262 at passage 34). The isochromosome i(1)(q10) in UOK 262 consists of two long arms of chromosome 1 fused together at the centromere region. We have repeated the FISH analysis for cells at both early and late passage (passages 6 and 63, respectively) and confirmed that UOK 262 cells contain isochromosome 1q i(1)(q10) as a clonal abnormality regardless of passage number.

Ten metaphase spreads were karyotyped by SKY, and each spread revealed multiple clonal abnormalities (Fig. 3D), as well as unique ones, and also multiple numerical and

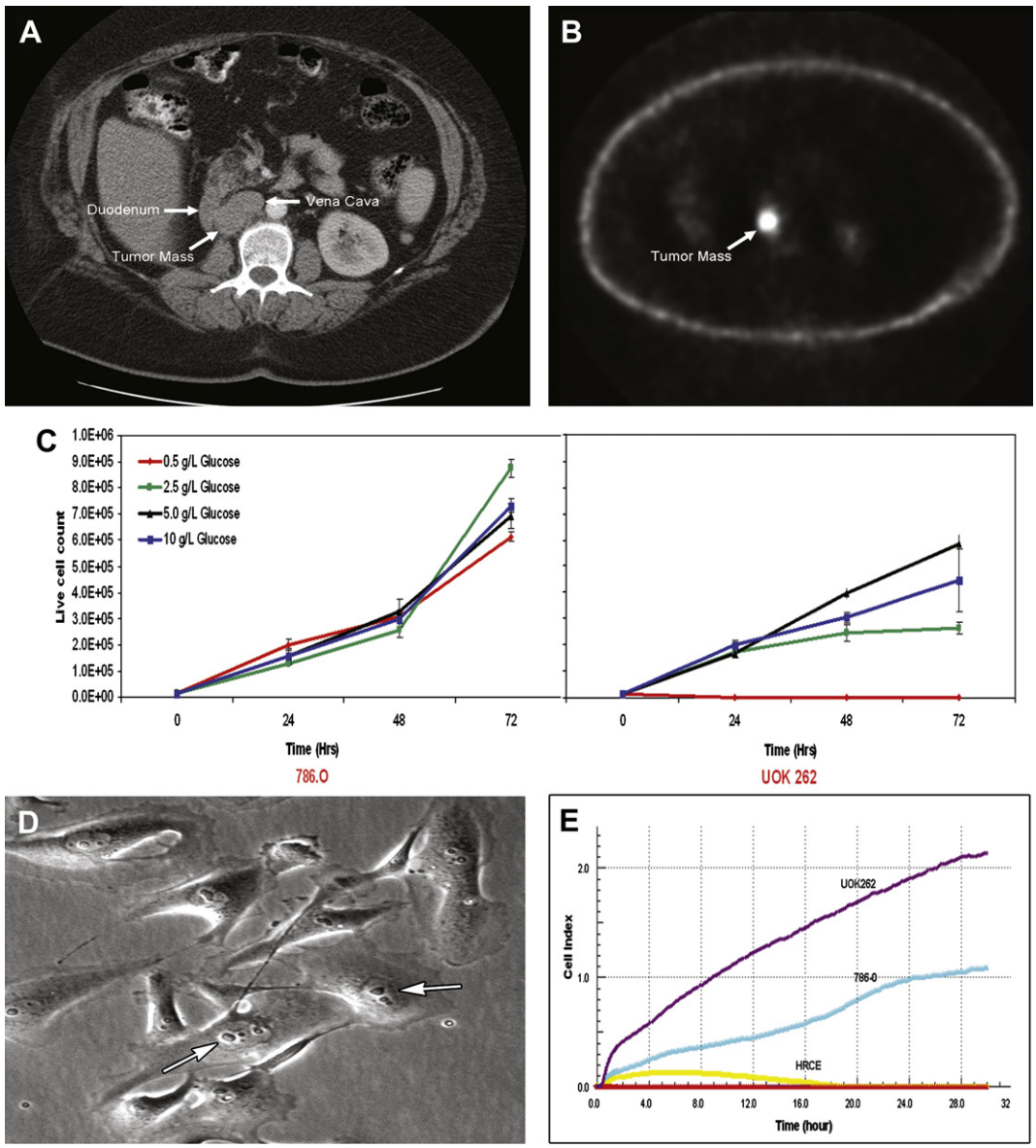

Fig. 1. (A) Abdominal computed tomography scan reveals a recurrent, right retroperitoneal tumor mass in a patient with hereditary leiomyomatosis renal cell carcinoma (HLRCC). (B) [^{18}F]fluorodeoxyglucose positron emission tomography imaging of the patient reveals strong glucose uptake in the lymph node tumor metastasis. (C) The in vitro growth of UOK 262 cells in 0.5, 2.5, 5, and 10 g/L D-glucose. Proliferation and survival of the cells were glucose dependent. (D) The morphology of UOK 262 cells in culture, showing active branching and the unique HLRCC pathological features of large nuclei with predominant nucleoli and atypical perinucleolar clearing (arrows) (40×). (E) Real-time assay of the invasive potential of UOK 262 cells, compared with control cells (786–O) and normal renal cortical epithelial cells (HRCE).

structural aberrations (indicative of genomic instability). The composite karyotype was 47,X,−X,+1,i(1)(q10),+5,der(21)t(15;21)(q15;p11.2),+22. The karyotype for UOK 262 has been entered into the NCBI SKY/CGH interactive online database (http://www.ncbi.nlm.nih.gov/sky/skyweb.cgi) [21,22]. Public access takes effect upon publication of the present article.

3.5. UOK 262 cells harbor an FH germline mutation at exon 8

The patient possessed a germline mutation in *FH* at nucleotide 1187 in exon 8, resulting in a Gln396Pro amino acid change (determined as previously described) [13]. To determine whether UOK 262 cells contain the identical *FH* germline mutation, we sequenced genomic DNA from early and late passages of the cell line. From the DNA sequencing chromatograms (Fig. 3A) we verified the nucleotide change as identical to the patient's germline missense mutation, which is an A to C change, in both early and late passages of UOK 262. Only the germline mutation sequence was present in the tumor cells, confirming a loss of heterozygosity of the wild-type allele at this nucleotide position. An amplified, single mutant allele is retained in UOK 262. (Figure 2C shows four copies of chromosome 1q in passage 34 cells.)

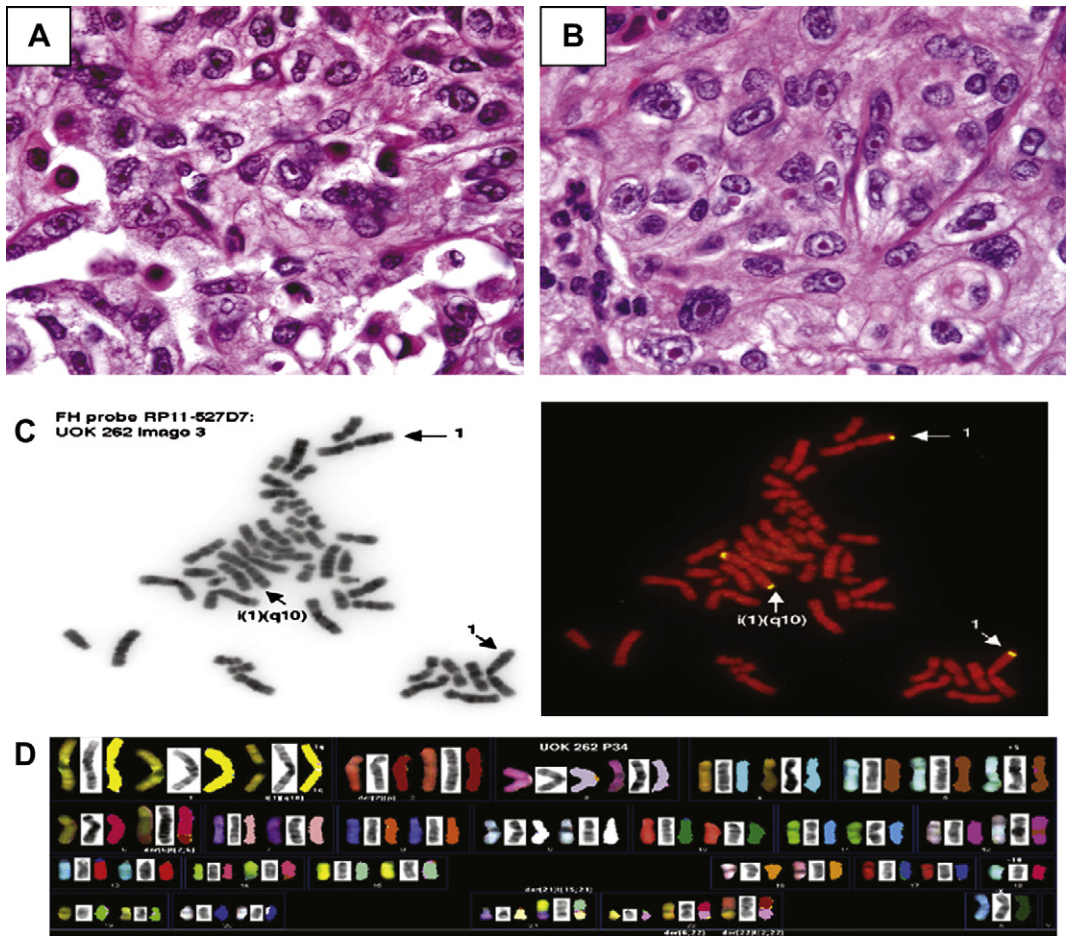

Fig. 2. (A) Tumor tissue from xenograft derived from UOK 262 cells (3×10^6). Hematoxylin–eosin (H&E) stain (original magnification: 200×). (B) H&E staining of tissue from metastatic HLRCC kidney cancer removed surgically from the patient's retroperitoneum (original magnification 200×). (C) Gene-specific fluorescence in situ hybridization (FISH) analysis of UOK 262 cells. The *FH* gene genomic probe RP11-527D7 (157 kb) is present in both normal copies of chromosome 1 and in an i(1)(q10), band 1q42.3. (D) Spectral karyotyping (SKY) revealed clonal and also multiple numerical and structural aberrations, for the composite karyotype 47,X,−X,+1,i(1)(q10), + 5,der(21)t(15;21)(q15;p11.2),+22.

3.6. Mitochondrial morphology, subcellular localization of mutant FH protein, and FH enzymatic activity in UOK 262

Ultrastructural examination of UOK 262 cells revealed a larger number of mitochondria in each cell than was seen in normal renal cortical epithelium cells (HRCE). Evaluation of UOK 262 mitochondria revealed edema, and various degrees of disintegration and disruption of the internal membrane cristae (Fig. 3B).

Recent reports [25,26] indicate that, in most human cells and tissues, FH protein is mainly or exclusively localized to the mitochondria. Having established that UOK 262 cells contain only a mutated version of the *FH* gene, we asked whether the predicted full-length mutant protein is present and localized in the mitochondria. Immunofluorescence was used to detect both FH and superoxide dismutase 2 (SOD2) (the mitochondrial form of the SOD protein family). The in situ distribution of both FH and SOD2 in UOK 262 (Fig. 4A) indicates that the mutant FH protein in UOK 262 is primarily colocalized with SOD2, confirming its presence in the mitochondrial matrix.

We further evaluated *FH* gene expression by real-time PCR and Western blot analysis, and we compared *FH* expression in UOK 262 cells to its expression in both 786–O and HK-2 renal cells. Although *FH* expression appears somewhat decreased in UOK 262 compared with the other cell lines (Fig. 4B, top and middle), Western blotting confirms that the expressed FH protein is full length, as predicted. Notably, the enzymatic activity of FH protein in UOK 262 cells is not detectable, and is at least 60-fold lower than in either 786–O or HK-2 cells (Fig. 4B, bottom).

3.7. UOK 262 cells overexpress genes and proteins involved in glycolysis

We initially examined whether glycolytic activity may be elevated in UOK 262 cells, using immunocytochemistry. UOK 262 cells were strongly positive for expression of the

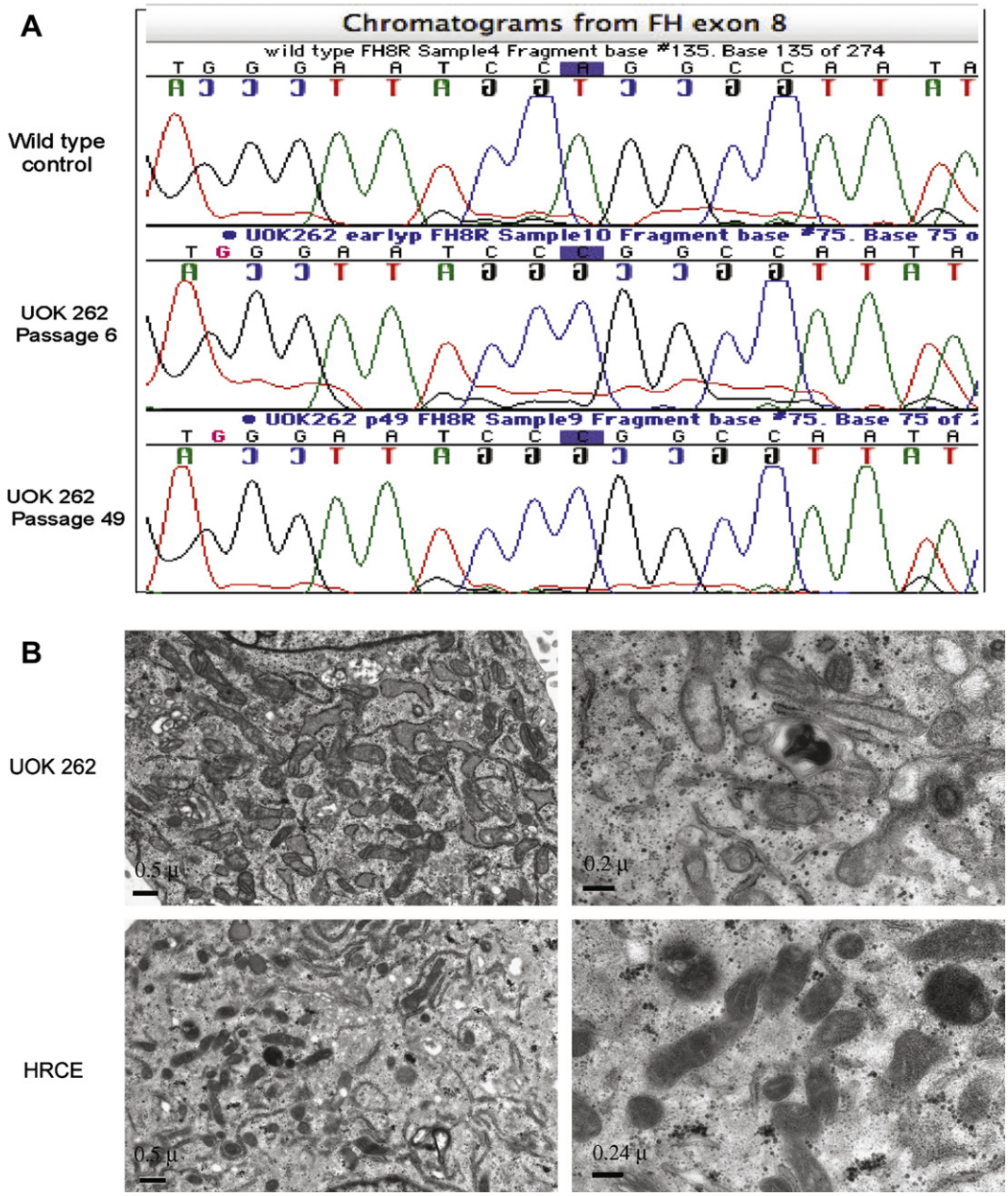

Fig. 3. (A) DNA chromatograms of the fumarate hydratase (*FH*) gene sequence surrounding nucleotide 1187. DNA was prepared from wild-type control sequence and early and late passages of UOK 262. (B) Transmission electron microscopy images of mitochondria from UOK 262 cells (top row) and from normal human renal cortical epithelial (HRCE) cells (bottom row). Mitochondria of UOK 262 tumor cells are edematous and show disruption of internal membrane cristae. Scale bars indicate magnification.

GLUT1 and LDHA proteins (Figs. 5A and 5B). We validated these data by determining mRNA expression using real-time PCR. We examined GLUT1 and LDHA expression, as well as expression of other mitochondrial enzymes and other proteins, including the Krebs cycle enzyme SDHC and, the master regulator of mitochondrial gene expression, PGC1A. In comparison with normal renal epithelium, we detected a twofold upregulation of PGC1A, greater than threefold upregulation of SDHC, and, consistent with our immunocytochemical data, ~15-fold upregulation of *LDHA* and >100-fold upregulation of *GLUT1* (Fig. 5C).

3.8. Significant attenuation of mitochondrial respiration in UOK 262 cells concomitant with increased glycolytic flux

We next explored the relative contributions of mitochondrial respiration, as measured by oxygen consumption rates (OCR), and glycolysis, as measured by extracellular acidification rate (ECAR), to energy production in UOK 262 cells. For comparison, we obtained similar data for 786–O and HK-2 cells. The basal OCR for UOK 262 cells was 21.98 ± 0.7 pmol/5×10^4 cells per minute; for HK-2 cells it was 89.46 ± 0.81 pmol/5×10^4 cells per minute; and for

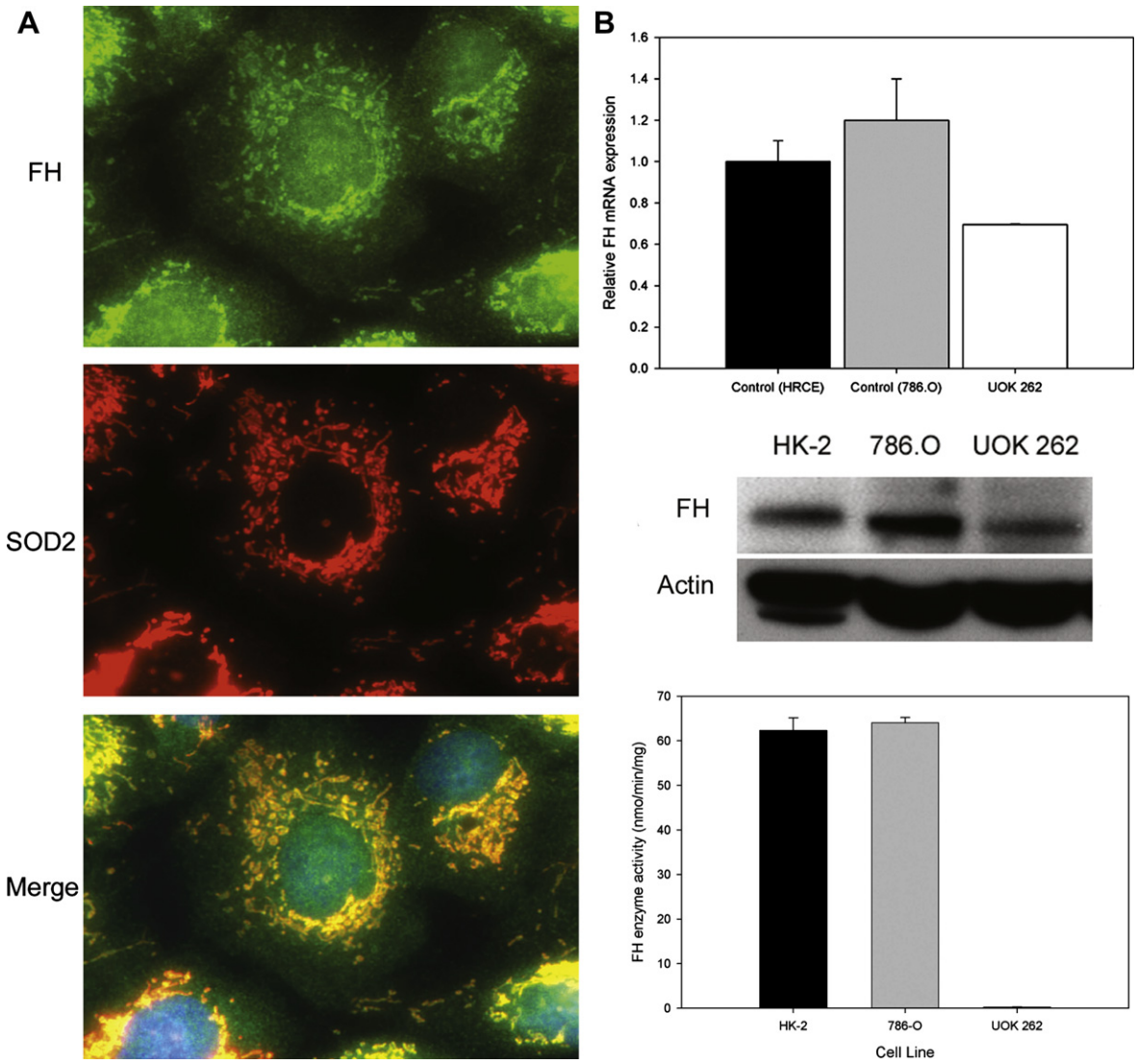

Fig. 4. (A) Double immunofluorescence labeling for protein expression in situ. Mutant FH protein is primarily localized to mitochondria of UOK 262 cells. Alexa-Fluor-488 labeling with mouse monoclonal antibody to human FH (top panel); Alexa Fluor-594 labeling with rabbit antibody to human superoxide dismutase 2 (SOD2), which is a marker of the mitochondria matrix (middle panel); and merge, or overlap of signals, obtained with both FH and SOD2 antibodies showing colocalization of FH and SOD2 (lower panel). (B) Real-time polymerase chain reaction (top panel) and Western blot (middle panel), showing that both mutant *FH* mRNA and protein are present in UOK 262 cells. FH enzymatic activity in UOK 262 cells (bottom panel) is undetectable.

786−O cells it was 195.98 ± 1.89 pmol/5 × 10^4 cells per minute (Fig. 5D). Based on instrument sensitivity, an OCR of ⩽20 pmol per minute is indistinguishable from signal noise, because of low levels of nonmitochondrial oxygen utilization: mitochondrial respiration accounts for ~ 90% of cellular oxygen consumption, and cellular protein oxidation accounts for the remaining 10% [27]. These data thus confirm that mitochondrial respiration is near zero in UOK 262 cells. By measuring ECAR in parallel with oxygen consumption, we found that glycolytic flux is markedly elevated in UOK 262, compared with the other cell lines (Fig. 5E), consistent with upregulation of LDHA, and with our recent study showing that these cells are obligate fermenters and must rely fully on glycolysis for energy production [28].

4. Discussion

In the 1920s, Otto Warburg made the remarkable observation that cancer cells preferentially use glycolysis to produce adenosine triphosphate, even in the presence of normal levels of oxygen (a phenomenon now known as the Warburg effect), and he proposed that abnormalities in energy metabolism were a fundamental aspect of cancer [15,29−31].

Hereditary leiomyomatosis renal cell carcinoma (HLRCC) is a novel form of inherited kidney cancer in which affected individuals are at risk for development of cutaneous and uterine leiomyomas and kidney cancer [1−3]. Characterized by germline inactivating mutation of the Krebs cycle enzyme fumarate hydratase [4], HLRCC is unique among kidney cancers in its remarkable

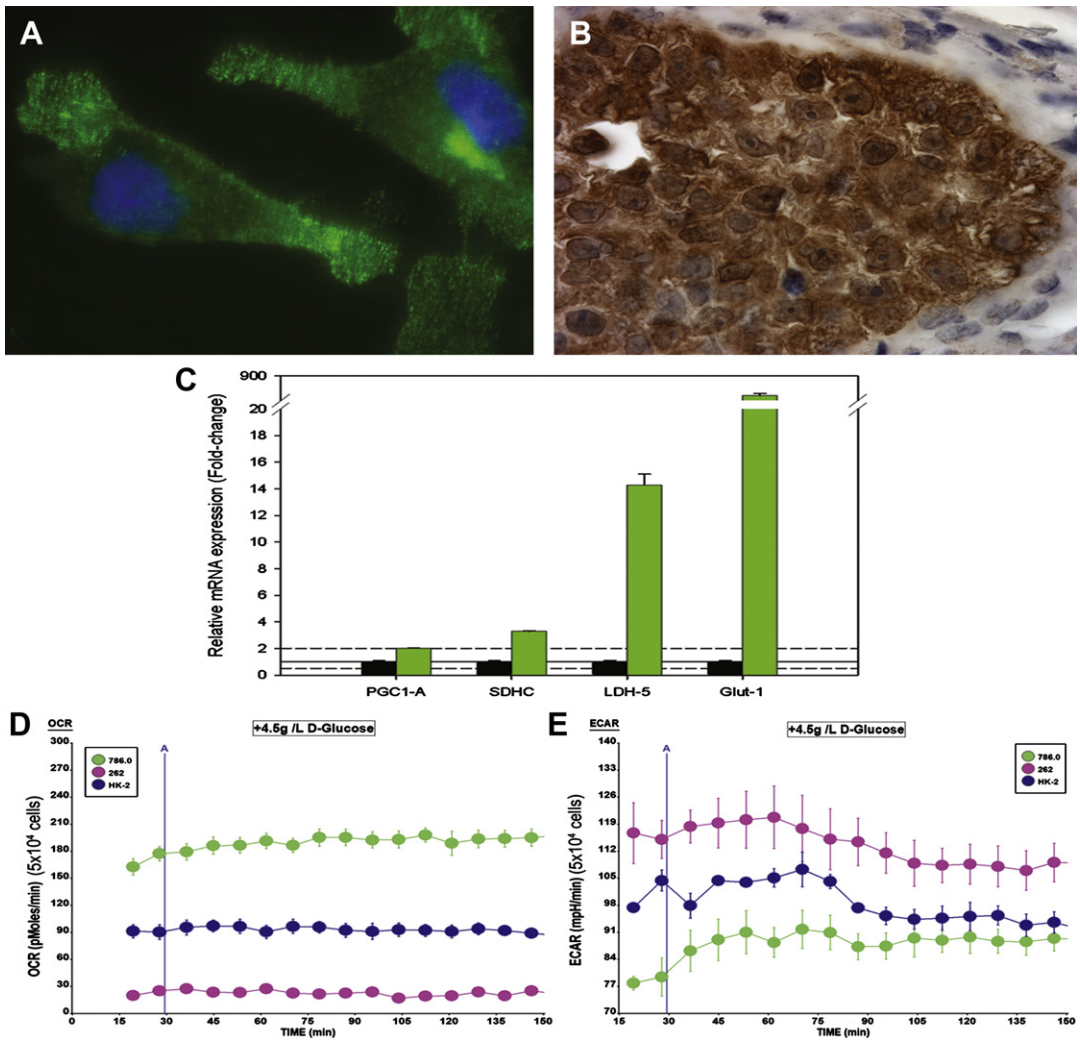

Fig. 5. Immunohistochemistry, real-time PCR analysis, and real-time measurement of mitochondrial respiration rate and lactate efflux (glycolysis rate) in UOK 262 cells. (A) GLUT1 protein is strongly expressed at branching tumor cell membrane (original magnification: 1000×); (B) LDHA is strongly expressed in a murine xenograft of UOK 262 cells (original magnification: 400×). (C) Comparison of gene expression in UOK 262 cells (green columns) with HRCE normal renal cortical epithelial cells (black columns). Note interruption in vertical scale [solid bar: no change line; dashed lines: twofold change up and down; error bars: standard error of the mean (SEM)]. (D) Basal cellular respiration rate (oxygen consumption rate, OCR) and (E) basal extracellular acidification rate (ECAR) of UOK 262 and control cells. Both OCR and ECAR were normalized against cell number and expressed as rate per 5×10^4 cells. Error bars indicate ± 1 standard deviation; $n = 5$.

propensity to grow quickly and metastasize early [6]. Detection of fumarate hydratase mutation in a high percentage of HLRCC families [4,13,32–33] has enabled early identification of disease in at-risk individuals, allowing for initiation of therapy when tumors are still small and potentially curable. Nonetheless, despite aggressive monitoring, patients remain at risk for the early development of advanced disease. The dependence of HLRCC tumors on glycolysis, coupled with their impaired mitochondrial respiration, mark this hereditary renal cancer as a unique example of Warburg's hypothesis [15]. The findings presented here suggest that strategies to interfere with glycolytic flux may represent a targeted approach to therapy for HLRCC.

Xie et al. [34] developed a novel A549 surrogate FH-deficient cell line that had increased lactate levels, enhanced HIF1A levels, and increased expression of GLUT1 and vascular endothelial growth factor (VEGF). Furthermore, Xie et al. [34] showed that LDH-A inhibition in the A549 FH-deficient cells increased apoptosis via reactive oxygen species (ROS) production and increased oxygen consumption.

The present article describes and characterizes UOK 262, a human cell line derived from a patient with HLRCC-associated kidney cancer. We recently showed glucose-mediated generation of cellular ROS and ROS-dependent HIF1A in UOK 262 [28]. We now report that that this cell line, which harbors an inactivating germline *FH* mutation and displays loss of heterozygosity, can grow as a xenograft in nude mice and exhibits additional notable characteristics: (a) autonomous growth that requires elevated extracellular glucose levels; (b) impaired oxidative phosphorylation; (c)

a highly invasive phenotype; (d) pronounced upregulation of genes involved in glucose uptake and metabolism; (e) and retention of the morphologic characteristics of HLRCC kidney cancer. UOK 262 thus provides a useful cell model for studying the underlying molecular derangements associated with impaired oxidative phosphorylation in cancer and for evaluating novel therapeutic approaches for this disease.

The majority of fatalities from HLRCC are caused by tumor invasion and metastasis. In the present case, FDG-PET scanning of the patient clearly imaged the metastatic, recurrent tumor. A tumor with constitutive impairment of mitochondrial respiration that is dependent on glucose transport and glycolysis for energy production is clearly imaged by FDG-PET imaging (an example of functional imaging). Overexpression of GLUT1, visualized by real-time PCR and immunohistochemistry, as well as the notable dependence of UOK 262 on high glucose for survival and proliferation, indicates that the in vitro model is phenotypically similar to HLRCC tumor tissue [9,34]. Whether the strong expression of glycolytic enzymes and enhanced glycolytic flux in UOK 262 is a direct consequence of loss of FH activity and resultant impairment of mitochondrial respiration is yet to be determined, but we and others have previously shown that molecular knockdown or knockout of FH in other cell lines leads to rapid upregulation of GLUT1 expression, glucose uptake, and glycolysis [9,34]. Furthermore, in a recent study we showed that these events are reversible upon reintroduction of functional FH, suggesting that lack of FH activity is sufficient to establish the phenotypic behavior of UOK 262 cells [28].

Isochromosome 1q frequently occurs in Wilms tumor and sarcomatoid tumors [35,36]. As we showed in our sequencing results in UOK 262 cells, only the germline mutant allele was retained, despite having four copies contained within the intact long arm of chromosome 1 (both homologues), as well as in the isochromosome i(1)(q10), that has two long arms of 1 fused at their centromeres (Fig. 2C). Isochromosome 1q may prove a marker for HLRCC. Zhang et al. [37] reported that chromosome-specific marker analysis from hereditary nonpolyposis colorectal cancer (HNPCC) indicated that loss of the wild-type allele predominantly occurs through locus-restricted recombinational events (i.e., gene conversion), rather than mitotic recombination or deletion of the respective gene locus. Of interest, if the extra copy number of chromosome arm 1q, including i(1)(q10), that contains the *FH* mutant allele is being selected for, it may have a role in UOK 262 tumorigenesis and in in vitro immortality. Alternatively, the absolute dependence of UOK 262 on glycolysis may itself determine the tumorigenicity and metastatic potential of these cells.

The morphology of mitochondria in UOK 262 cells suggests that mitochondrial function may be impaired and that the mitochondrial membrane or matrix may be disrupted. In UOK 262, mutant FH protein was targeted to mitochondria, and it was strongly associated with the mitochondrial matrix. Whether the mitochondrial localization of enzymatically inactive FH plays a role in the mitochondrial swelling and cristae disruption seen in UOK 262 is currently being investigated.

In summary, the fumarate hydratase deficient (FH^{-}/FH^{-}) UOK 262 kidney cancer cell line represents a genetically defined example of the Warburg phenomenon in a human cancer. It provides both an opportunity to study the molecular pathways that are deregulated in cancer when mitochondrial respiration is compromised and also a platform for testing novel therapeutic strategies that target energy deregulation in human cancer.

Acknowledgments

This research was supported by the Intramural Research Program of the U.S. National Institutes of Health, National Cancer Institute, Center for Cancer Research. We thank Robert A. Worrell, PhD, for operative tissue procurement; Linda Stapleton-Barenboim, for preparation of the SKY probes**;** Guofeng Zhang, PhD, for processing electron microscopy thin sections and images acquisitions; Catherine Wells, for assistance with animal xenograft studies; and Georgia Shaw, for editorial support.

References

[1] Fernández-Pugnaire MA, Delgado-Florencio V. Familial multiple cutaneous leiomyomas. Dermatology 1995;191:295–8.

[2] Zbar B, Glenn G, Lubensky I, Choyke P, Walther MM, Magnusson G, Bergerheim US, Pettersson S, Amin M, Hurley K. Hereditary papillary renal cell carcinoma: clinical studies in 10 families. J Urol 1995; 153:907–12.

[3] Launonen V, Vierimaa O, Kiuru M, Isola J, Roth S, Pukkala E, Sistonen P, Herva R, Aaltonen LA. Inherited susceptibility to uterine leiomyomas and renal cell cancer. Proc Natl Acad Sci U S A 2001; 98:3387–92.

[4] Tomlinson IP, Alam NA, Rowan AJ, Barclay E, Jaeger EE, Kelsell D, Leigh I, Gorman P, Lamlum H, Rahman S, Roylance RR, Olpin S, Bevan S, Barker K, Hearle N, Houlston RS, Kiuru M, Lehtonen R, Karhu A, Vilkki S, Laiho P, Eklund C, Vierimaa O, Aittomäki K, Hietala M, Sistonen P, Paetau A, Salovaara R, Herva R, Launonen V, Aaltonen LA. Multiple Leiomyoma Consortium. Germline mutations in *FH* predispose to dominantly inherited uterine fibroids, skin leiomyomata and papillary renal cell cancer. Nat Genet 2002;30:406–10.

[5] Kiuru M, Lehtonen R, Arola J, Salovaara R, Järvinen H, Aittomäki K, Sjöberg J, Visakorpi T, Knuutila S, Isola J, Delahunt B, Herva R, Launonen V, Karhu A, Aaltonen LA. Few *FH* mutations in sporadic counterparts of tumor types observed in hereditary leiomyomatosis and renal cell cancer families. Cancer Res 2002;62:4554–7.

[6] Grubb RL 3rd, Franks ME, Toro J, Middelton L, Choyke L, Fowler S, Torres-Cabala C, Glenn GM, Choyke P, Merino MJ, Zbar B, Pinto PA, Srinivasan R, Coleman JA, Linehan WM. Hereditary leiomyomatosis and renal cell cancer: a syndrome associated with an aggressive form of inherited renal cancer. J Urol 2007;177:2074–9.

[7] Kiuru M, Launonen V, Hietala M, Aittomäki K, Vierimaa O, Salovaara R, Arola J, Pukkala E, Sistonen P, Herva R, Aaltonen LA. Familial cutaneous leiomyomatosis is a two-hit condition associated with renal cell cancer of characteristic histopathology. Am J Pathol 2001;159:825–9.

[8] Merino MJ, Torres-Cabala C, Pinto P, Linehan WM. The morphologic spectrum of kidney tumors in hereditary leiomyomatosis and renal cell carcinoma (HLRCC) syndrome. Am J Surg Pathol 2007;31:1578–85.

[9] Isaacs JS, Jung YJ, Mole DR, Lee S, Torres-Cabala C, Chung YL, Merino M, Trepel J, Zbar B, Toro J, Ratcliffe PJ, Linehan WM, Neckers L. HIF overexpression correlates with biallelic loss of fumarate hydratase in renal cancer: novel role of fumarate in regulation of HIF stability. Cancer Cell 2005;8:143–53.

[10] Pollard PJ, Brière JJ, Alam NA, Barwell J, Barclay E, Wortham NC, Hunt T, Mitchell M, Olpin S, Moat SJ, Hargreaves IP, Heales SJ, Chung YL, Griffiths JR, Dalgleish A, McGrath JA, Gleeson MJ, Hodgson SV, Poulsom R, Rustin P, Tomlinson IP. Accumulation of Krebs cycle intermediates and over-expression of HIF1α in tumours which result from germline *FH* and *SDH* mutations. Hum Mol Genet 2005;14:2231–9.

[11] Matyakhina L, Freedman RJ, Bourdeau I, Wei MH, Stergiopoulos SG, Chidakel A, Walther M, Abu-Asab M, Tsokos M, Keil M, Toro J, Linehan WM, Stratakis CA. Hereditary leiomyomatosis associated with bilateral, massive, macronodular adrenocortical disease and atypical Cushing syndrome: a clinical and molecular genetic investigation. J Clin Endocrinol Metab 2005;90:3773–9.

[12] Alam NA, Olpin S, Leigh IM. Fumarate hydratase mutations and predisposition to cutaneous leiomyomas, uterine leiomyomas and renal cancer. Br J Dermatol 2005;153:11–7.

[13] Wei MH, Toure O, Glenn GM, Pithukpakorn M, Neckers L, Stolle C, Choyke P, Grubb R, Middelton L, Turner ML, Walther MM, Merino MJ, Zbar B, Linehan WM, Toro JR. Novel mutations in *FH* and expansion of the spectrum of phenotypes expressed in families with hereditary leiomyomatosis and renal cell cancer. J Med Genet 2006;43:18–27.

[14] Arany Z, Foo SY, Ma Y, Ruas JL, Bommi-Reddy A, Girnun G, Cooper M, Laznik D, Chinsomboon J, Rangwala SM, Baek KH, Rosenzweig A, Spiegelman BM. HIF-independent regulation of VEGF and angiogenesis by the transcriptional coactivator PGC-1α. Nature 2008;451:1008–12.

[15] Warburg O. On the origin of cancer cells. Science 1956;123:309–14.

[16] Anglard P, Trahan E, Liu S, Latif F, Merino MJ, Lerman MI, Zbar B, Linehan WM. Molecular and cellular characterization of human renal cell carcinoma cell lines. Cancer Res 1992;52:348–56.

[17] Yang Y, Padilla-Nash HM, Vira MA, Abu-Asab MS, Val D, Worrell R, Tsokos M, Merino MJ, Pavlovich CP, Ried T, Linehan WM, Vocke CD. The UOK 257 cell line: a novel model for studies of the human Birt–Hogg–Dubé gene pathway. Cancer Genet Cytogenet 2008;180:100–9.

[18] Shipley JM, Birdsall S, Clark J, Crew J, Gill S, Linehan M, Gnarra J, Fisher S, Craig IW, Cooper CS. Mapping the X chromosome breakpoint in two papillary renal cell carcinoma cell lines with a t(X;1)(p11.2;q21.2) and the first report of a female case. Cytogenet Cell Genet 1995;71:280–4.

[19] Sidhar SK, Clark J, Gill S, Hamoudi R, Crew AJ, Gwilliam R, Ross M, Linehan WM, Birdsall S, Shipley J, Cooper CS. The t(X;1)(p11.2;q21.2) translocation in papillary renal cell carcinoma fuses a novel gene *PRCC* to the *TFE3* transcription factor gene. Hum Mol Genet 1996;5:1333–8.

[20] Wu M, Neilson A, Swift AL, Moran R, Tamagnine J, Parslow D, Armistead S, Lemire K, Orrell J, Teich J, Chomicz S, Ferrick DA. Multiparameter metabolic analysis reveals a close link between attenuated mitochondrial bioenergetic function and enhanced glycolysis dependency in human tumor cells. Am J Physiol Cell Physiol 2007;292:C125–36.

[21] Padilla-Nash HM, Barenboim-Stapleton L, Difilippantonio MJ, Ried T. Spectral karyotyping analysis of human and mouse chromosomes. Nat Protoc 2006;1:3129–42.

[22] Shaffer LG, Tommerup N, editors. ISCN 2005: an international system for human cytogenetic nomenclature (2005). Basel: S. Karger, 2005.

[23] Smith PK, Krohn RI, Hermanson GT, Mallia AK, Gartner FH, Provenzano MD, Fujimoto EK, Goeke NM, Olson BJ, Klenk DC. Measurement of protein using bicinchoninic acid [Erratum in: Anal Biochem 1987;163:279]. Anal Biochem 1985;150:76–85.

[24] Hatch MD. A simple spectrophotometric assay for fumarate hydratase in crude tissue extracts. Anal Biochem 1978;85:271–5.

[25] Singh B, Gupta RS. Mitochondrial import of human and yeast fumarase in live mammalian cells: retrograde translocation of the yeast enzyme is mainly caused by its poor targeting sequence. Biochem Biophys Res Commun 2006;346:911–8.

[26] Bowes T, Singh B, Gupta RS. Subcellular localization of fumarase in mammalian cells and tissues. Histochem Cell Biol 2007;127:335–46.

[27] Ferrick DA, Neilson A, Beeson C. Advances in measuring cellular bioenergetics using extracellular flux. Drug Discov Today 2008;13:268–74.

[28] Sudarshan S, Sourbier C, Kong HS, Block K, Valera Romero VA, Yang Y, Galindo C, Mollapour M, Scroggins B, Goode N, Lee MJ, Gourlay CW, Trepel J, Linehan WM, Neckers L. Fumarate hydratase deficiency in renal cancer induces glycolytic addiction and hypoxia-inducible transcription factor 1α stabilization by glucose-dependent generation of reactive oxygen species. Mol Cell Biol 2009;29:4080–90.

[29] Warburg O, Posener K, Negelein E. Metabolism of the carcinoma cell [In German]. Biochem Z 1924;152:309–44.

[30] Garber K. Energy deregulation: licensing tumors to grow. Science 2006;312:1158–9.

[31] Shaw RJ. Glucose metabolism and cancer. Curr Opin Cell Biol 2006;18:598–608.

[32] Alam NA, Rowan AJ, Wortham NC, Pollard PJ, Mitchell M, Tyrer JP, Barclay E, Calonje E, Manek S, Adams SJ, Bowers PW, Burrows NP, Charles-Holmes R, Cook LJ, Daly BM, Ford GP, Fuller LC, Hadfield-Jones SE, Hardwick N, Highet AS, Keefe M, MacDonald-Hull SP, Potts ED, Crone M, Wilkinson S, Camacho-Martinez F, Jablonska S, Ratnavel R, MacDonald A, Mann RJ, Grice K, Guillet G, Lewis-Jones MS, McGrath H, Seukeran DC, Morrison PJ, Fleming S, Rahman S, Kelsell D, Leigh I, Olpin S, Tomlinson IP. Genetic and functional analyses of *FH* mutations in multiple cutaneous and uterine leiomyomatosis, hereditary leiomyomatosis and renal cancer, and fumarate hydratase deficiency. Hum Mol Genet 2003;12:1241–52.

[33] Toro JR, Nickerson ML, Wei MH, Warren MB, Glenn GM, Turner ML, Stewart L, Duray P, Tourre O, Sharma N, Choyke P, Stratton P, Merino M, Walther MM, Linehan WM, Schmidt LS, Zbar B. Mutations in the fumarate hydratase gene cause hereditary leiomyomatosis and renal cell cancer in families in North America. Am J Hum Genet 2003;73:95–106.

[34] Xie H, Valera VA, Merino MJ, Amato AM, Signoretti S, Linehan WM, Sukhatme VP, Seth P. LDH-A inhibition, a therapeutic strategy for treatment of hereditary leiomyomatosis and renal cell cancer. Mol Cancer Ther 2009;8:626–35.

[35] Mertens F, Johansson B, Mitelman F. Isochromosomes in neoplasia. Genes Chromosomes Cancer 1994;10:221–30.

[36] Mitelman F, Johansson B, Mertens F, editors. Catalog of chromosome aberrations in cancer. 5th ed. New York: Wiley-Liss, 1994.

[37] Zhang J, Lindroos A, Ollila S, Russell A, Marra G, Mueller H, Peltomaki P, Plasilova M, Heinimann K. Gene conversion is a frequent mechanism of inactivation of the wild-type allele in cancers from *MLH1*/*MSH2* deletion carriers. Cancer Res 2006;66:659–64.